

Novel 4-Vinylpyridine-Extended Metal–Dibenzoylmethanate Host Frameworks: Structure, Polymorphism, and Inclusion Properties**[†]

Dmitriy V. Soldatov^[a, b] and John A. Ripmeester^{*[a]}

Abstract: In this contribution we show that host materials based on metal dibenzoylmethanates (DBM) can be extended in a versatile way by decreasing the packing efficiency of the simpler metal DBM's reported earlier. Specifically, this can be accomplished by coordinating two 4-vinylpyridines (4-ViPy) to the metal (Ni or Co) DBM units to give $[M(4\text{-ViPy})_2(\text{DBM})_2]$ host complexes. These display a remarkable polymorphism and an ability to form inclusion compounds with a large variety of organic species. Five non-clathrate phases representing three polymorphic types and twenty-eight inclusion compounds with nineteen guests representing five structural types were isolated and studied in varying degrees of detail. The inclusion compounds can be prepared

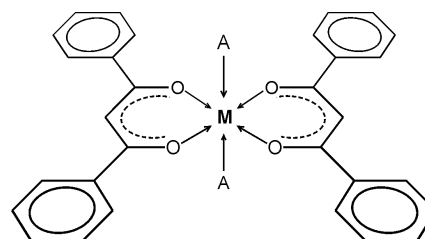
by recrystallization or by interaction of the solid host with guest vapor. In the latter case, the process realization, kinetics and final product strongly depend on the host polymorph chosen as starting material. Kinetic studies executed with powder XRD suggest that transient formation of inclusion compounds may occur even during solvent vapor induced transformation of one guest-free polymorph to another. The β polymorph of the Ni-host reveals the strongest clathratogenic ability as well as a high selectivity towards certain homologues

Keywords: host–guest systems • inclusion compounds • polymorphism • supramolecular chemistry • zeolite analogues

and isomers. Its properties give insight into the concept of “flexible zeolite mimics”, or “apohosts”, as this empty host form is energetically and structurally predisposed towards inclusion processes. In all eleven (three host and eight clathrate) structures studied by single crystal X-ray diffraction the $[M(4\text{-ViPy})_2(\text{DBM})_2]$ complex molecule is *trans*-configured. In most, the host molecules show effective packing in one dimension by forming parallel chains. Guest species are located between the chains in cages or channels formed by combining voids in the host molecules belonging to adjacent chains. The corresponding Ni and Co versions of the compounds studied were similar.

Introduction

The *trans*-configured metal(II) dibenzoylmethanate fragment (Scheme 1) is an electrically neutral lozenge-like unit that has a rather rigid center where the two dibenzoylmethanate (hereinafter DBM) ligands chelate to the metal center in the equatorial plane, but that has some flexibility due to rotational freedom of the phenyl moieties on the periphery. Modified by introducing appropriate axial ligands A, the complex acquires the ability to entrap solvent species to give a



Scheme 1. General formula (M, metal; A, ligand).

number of inclusion structures of varied topology and stoichiometry.^[1, 2] Although other metal bis-chelates have been utilized for the construction of porous solids, these usually do not maintain their host properties upon extensive modification.^[3–5]

The $[\text{NiPy}_2(\text{DBM})_2]$ host (Scheme 1, $M = \text{Ni}^{\text{II}}$, $A = \text{pyridine}$) was found to form four structural types with the six guests used.^[1] These inclusions show van der Waals packing with the guest species included in cages or channels of various topologies. The title $[M(4\text{-ViPy})_2(\text{DBM})_2]$ hosts (4-ViPy = 4-

[a] Dr. J. A. Ripmeester, Dr. D. V. Soldatov
Steele Institute for Molecular Sciences
National Research Council of Canada
100 Sussex, K1A 0R6 Ottawa (Canada)
Fax: (+1) 613 998-7833
E-mail: jar@ned1.sims.nrc.ca

[b] Dr. D. V. Soldatov
Permanent address: Institute of Inorganic Chemistry, Lavrentyeva 3
Novosibirsk 630090 (Russia)

[**] Part III, Series Title: “Modified metal dibenzoylmethanates and their clathrates”; for Parts I and II see: refs. [1] and [2].

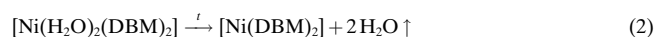
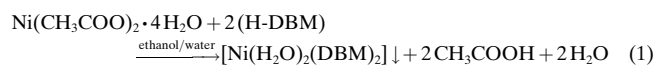
[†] Issued as NRCC No. 43881

vinylpyridine), bearing Ni and Co centers, were shown to form inclusions with carbon tetrachloride (of the cage type) and chlorobenzene (of the channel type).^[2] In the present work we elucidate the polymorphism of the complexes themselves as well as their versatile inclusion properties with a number of volatile guests, and discuss the extension of the axial amine ligands as a strategy for generating versatile new families of host materials. The work also sheds light on the nature and role of “apohosts”, polymorphs that do not have obvious pore space, but that are pre-organized to transform to clathrates upon exposure to guest vapor.

Experimental Section

Preparations

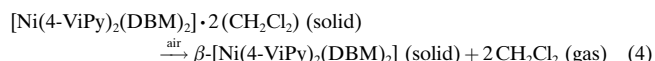
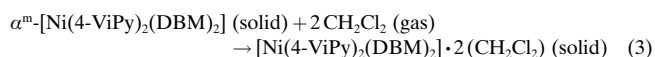
Bis(dibenzoylmethanato)nickel(II), [Ni(DBM)₂]: This complex salt was prepared in two steps [Eqs. (1)–(2)], comprising the synthesis of a diaquo-complex^[6] and thermal dehydration, similar to the method with the diammonium complex reported previously.^[1] Into a hot solution of nickel acetate tetrahydrate (2.49 g, 10 mmol) in 90% ethanol (150 mL) a solution of dibenzoylmethane, C₆H₅COCH₂COC₆H₅, (Aldrich, 98%; 4.49 g, 20 mmol) in 90% ethanol (150 mL) was added all at once. The mixture was allowed to cool for at least 1 h while stirring. A light-green crystalline precipitate was separated, rinsed with 90% ethanol, and air-dried to give the diaquo-complex (ca. 5.1 g, 95%). This was dehydrated for 2 h at 130 °C to give a yellow-green final product; a mass loss of 7.0 to 7.3% was observed as compared to a value of 6.7% calculated from Equation (2). Elemental analysis (%) calcd for [Ni(DBM)₂] (C₃₀H₂₂NiO₄): C 71.3, H 4.39; found: C 71.5, H 4.34.



Bis(dibenzoylmethanato)cobalt(II), [Co(DBM)₂]: The method was very similar to that for the nickel analogue; dehydration of the orange diaquo-complex for 1 h at 120 °C (mass loss of 7.1 to 7.2%) yielded dark-yellow final product. Elemental analysis (%) calcd for [Co(DBM)₂] (C₃₀H₂₂CoO₄): C 71.3, H 4.39; found: C 71.4, H 4.40.

α^m -Bis(4-vinylpyridine)bis(dibenzoylmethanato)nickel(II), α^m -[Ni(4-ViPy)₂(DBM)₂]: [Ni(DBM)₂] (2.5 g, 5 mmol) was dissolved in warm tetrahydrofuran (50 mL), and the bright-green filtrate was cooled to room temperature, then poured into a solution of 4-vinylpyridine (Aldrich, 95%; 1.6 g, 15 mmol) in absolute ethanol (250 mL). After stirring for 30 min the yellow-green fine-crystalline product was separated, rinsed with ethanol, and air-dried (80% yield from nickel dibenzoylmethanate). Elemental analysis (%) calcd for [Ni(4-ViPy)₂(DBM)₂] (C₄₄H₃₆N₂NiO₄): C 73.9, H 5.07, N 3.92; found: C 74.1, H 5.06, N 3.84. A powder X-ray test indicated the presence of only the stable α^m polymorph of the complex (Figure 1b).

β -Bis(4-vinylpyridine)bis(dibenzoylmethanato)nickel(II), β -[Ni(4-ViPy)₂(DBM)₂]: The preparation was completed in two steps [Eqs. (3)–(4)] using methylene chloride as template. A weighed sample of α^m -[Ni(4-ViPy)₂(DBM)₂] (1.4 g, 2 mmol) was placed in an atmosphere of methylene chloride for several hours until a weight increase of ca. 24% (corresponding to 1:2 complex per methylene chloride mole ratio) was observed. After one more hour the sample was removed from the methylene chloride atmosphere and left overnight in a flow of air until the sample returned to its initial mass. Elemental analysis (%) calcd for [Ni(4-ViPy)₂(DBM)₂] (C₄₄H₃₆N₂NiO₄): C 73.9, H 5.07, N 3.92; found: C 73.5, H 4.85, N 3.72. A powder X-ray test indicated the presence of the pure β polymorph of the complex (Figure 1d). In air, this metastable polymorph remains intact for at least five months, but relaxes in minutes to the stable α^m polymorph upon heating or upon being exposed to certain organic solvent vapors (see Results and Discussion).



α^m -Bis(4-vinylpyridine)bis(dibenzoylmethanato)cobalt(II), α^m -[Co(4-ViPy)₂(DBM)₂]: [Co(DBM)₂] (2.5 g, 5 mmol) was dissolved in a mixture of 4-vinylpyridine (Aldrich, 95%; 1.6 g, 15 mmol) and chloroform (30 mL). The dark-red solution was filtered and poured into absolute ethanol (250 mL). After stirring for 20 min the orange-red fine-crystalline product was separated, rinsed with ethanol, and air-dried (75% yield from cobalt dibenzoylmethanate). Elemental analysis (%) calcd [Co(4-ViPy)₂(DBM)₂] (C₄₄H₃₆CoN₂O₄): C 73.8, H 5.07, N 3.91; found: C 73.5, H 4.79, N 3.78. Powder X-ray control is necessary (Figure 1c). This metastable polymorph may be kept in air but transforms to the stable α' polymorph of the complex in an atmosphere of many organic solvents (see Results and Discussion).

α' -Bis(4-vinylpyridine)bis(dibenzoylmethanato)cobalt(II), α' -[Co(4-ViPy)₂(DBM)₂]: This polymorph of the complex which is stable was prepared in the course of prolonged stirring of metastable α^m -[Co(4-ViPy)₂(DBM)₂] (1 g) in absolute ethanol (100 mL). With a small quantity of nucleation agent added, the process was complete in 5 h. Elemental analysis (%) calcd for [Ni(4-ViPy)₂(DBM)₂] (C₄₄H₃₆N₂NiO₄): C 73.9, H 5.07, N 3.92; found: C 73.6, H 4.99, N 3.59. Quality control by powder X-ray diffraction is necessary (Figure 1a).

β -Bis(4-vinylpyridine)bis(dibenzoylmethanato)cobalt(II), β -[Co(4-ViPy)₂(DBM)₂]: As observable from powder X-ray tests (Figure 1e; isomorphous to the Ni-form, pattern d), this polymorph formed during the first moments upon fast decomposition of the inclusion with methylene chloride, [Co(4-ViPy)₂(DBM)₂] · 2(CH₂Cl₂), analogously to the Ni-compound [Eq. (4)]. However, unlike the latter, the β -[Co(4-ViPy)₂(DBM)₂] decomposed quickly to give one of the α -modifications, or a mixture of the two.

Host and inclusion compounds by crystallization: To prepare crystalline products and single crystals for X-ray diffraction experiments, host complexes in the α^m form and neat solvents were used. If the solubility was low, solutions saturated at 40 °C were filtered and left to cool, otherwise, slow evaporation at room temperature was used. Crystals of inclusion compounds usually were kept under their mother liquors. The solvents used and the crystallization products assigned according to X-ray unit cell measurement on randomly chosen crystals, are listed in Tables 1 to 3. Crystals of metastable α^m -[Co(4-ViPy)₂(DBM)₂] were obtained upon evaporating a toluene solution.

Isopiestic experiments: Samples of \approx 100 mg of host polymorphs were placed in closed vessels in an atmosphere of the appropriate guest. Saturated solutions of the host complex in the corresponding guest liquid were used to maintain the guest vapor pressure which is equal to the equilibrium guest pressure over the expected inclusion with maximum guest content. Excess absorbed solvent was removed periodically by gentle airing and the absorption process was continued until constant mass was achieved. More details on the technique were provided earlier.^[4]

Two or more independent determinations were made. Compositions x of the reaction products were calculated from the formula $x = (\Delta m/m_0)(M_H/M_G)$, where Δm and m_0 are the mass increase and the starting sample mass, and M_H and M_G are host and guest molecular masses, respectively. If no significant increase in sample mass was observed in three weeks, the samples were recovered anyway. The final product was then analyzed by the X-ray powder diffraction method wherefrom it was assigned to one of the host polymorphs or the inclusion structural types (Figure 1).

Methods

Analyses: Complexes including various host polymorphs were analyzed with a LECO CHN-1000 Analyser; three determinations with 100 mg samples were done in each case. Compositions for inclusions were determined from isopiestic measurements as described above. Phase analyses were performed with powder samples on a Rigaku Geigerflex diffractometer (CoK α radiation, $\lambda = 1.7902 \text{ \AA}$) in a 5–15° 2 θ range, 0.02° step scan with 1 or 2 s per step. Samples recovered after isopiestic experiments were studied in an atmosphere of the corresponding guest.

Single-crystal diffraction analysis: Single crystals, or pieces cut therefrom, were taken from under their respective mother liquors and cooled immediately to –100 °C, at which temperature all further experiments

were done. A Bruker SMART CCD X-ray diffractometer with graphite-monochromated $\text{MoK}\alpha$ radiation ($\lambda = 0.7107 \text{ \AA}$) was used to collect diffraction data. Preliminary unit cell parameters were determined using 60 or more frame ω scans, 0.3° wide, starting at three different φ positions. Full data sets were collected using the ω scan mode over the 2θ range of $3-58^\circ$. Coverage of the unique sets was over 96%. An empirical absorption correction utilized the SADABS routine associated with the Bruker diffractometer. The final unit cell parameters were obtained using the entire data set.

The structures were solved and refined using the SHELXTL package^[7] using direct methods followed by differential Fourier syntheses. The structural refinement was performed on F^2 using all data with positive intensities. Non-hydrogen atoms were refined anisotropically. Isotropic approximations and geometric constraints were applied in some cases for minor orientations of vinyl groups or guest molecules. Hydrogen atoms were refined isotropically with thermal factors 1.2 or 1.5 times greater than those for the adjacent carbon atoms. Site occupancy factors for guest orientations were refined independently; in the last cycles their sums were fixed to give the ideal stoichiometry as observed deviations were not significant (see Tables 2 and 3). The largest residual extrema on the final difference map were located about the heavy atoms (Cl, Co, Ni).

Analysis of packing and preparation of illustrations were accomplished using XP^[7], CLAT^[8] and Raster3D^[9] program packages. The following values for van der Waals radii were applied:^[10] C 1.71, H 1.16, Cl 1.90, N 1.52, O 1.29, Co 1.50, Ni 1.63 \AA .

A summary of the crystal data and experimental parameters is given in Table 1. Crystallographic data (excluding structure factors) for the structures reported in this paper have been deposited with the Cambridge Crystallographic Data Centre as supplementary publication no. CCDC-150623 to 150638, the numbers given in Table 1. Copies of the data can be obtained free of charge on application to CCDC, 12 Union Road,

Cambridge CB21EZ, UK (fax: (+44) 1223-336-033; e-mail: deposit@ccdc.cam.ac.uk).

DSC Measurements: These were performed using a 2920 modulated differential scanning calorimeter (TA Instruments). Samples of 5 to 10 mg were pressed into aluminum pans and the DSC curves were recorded at a 5° per min heating rate. Two determinations were made for each polymorph using samples from two independent syntheses, and the calorimeter was calibrated before each run.

Determination of kinetic curves: For kinetic experiments a Rigaku Geigerflex diffractometer ($\text{CoK}\alpha$ radiation, $\lambda = 1.7902 \text{ \AA}$) equipped with a hermetic reaction camera was adapted to determine in situ phase interconversions. The sample (ca. 20 mg) of pure β -host phase was placed in a brass holder as a layer of 0.25 mm in depth. The holder then was placed in the camera in an atmosphere of the required solvent and diffractograms were recorded periodically in the $9-12^\circ$ 2θ -range (<3 min per one diffractogram). In this range (Figure 1) the α^m -host phase shows as three peaks at 2θ angles of 9.76 , 11.29 and 11.48° , the β -host phase as three peaks at 10.17 , 10.81 and 11.41° , and the clathrate phase (MC type) at 9.84 , 10.20 and 11.63° . The integral intensities of four segments of an experimental diffractogram (with subtracted background) were taken for calculating a distribution of the three phases in a given sample: segment 1, $9.3-10^\circ$; segment 2, $10-10.4^\circ$; segment 3, $10.4-11^\circ$; segment 4, $11-11.8^\circ$. Then the system of four linear equations $X \times X_{0i} + Y \times Y_{0i} + Z \times Z_{0i} = I_i$ (where X, Y, and Z are the fractions of α^m , β and the clathrate phases in the sample studied, respectively; i is the number of the segment, X_{0i} , Y_{0i} and Z_{0i} are intensities for the i^{th} segment for the pure α^m , β and clathrate phases; I_i is the intensity of the i^{th} segment observed in the experiment) was solved using a minimization procedure and the $X+Y+Z=1$ condition. The minimization was accomplished using the option SOLVER of the Microsoft Excel program, where the sum of the squared differences between observed and calculated intensities for four segments was minimized.

Table 1. Crystal data and X-ray experiment details for the $[\text{M}(4\text{-ViPy})_2(\text{DBM})_2]$ polymorphs and inclusion compounds (assumed values are given in brackets).

Host (M)	Co	Ni	Co	Ni	Co	Ni
Guest	no	no	no	C_6H_6	C_6H_6	CH_2Cl_2
host:guest ratio	–	–	–	1:1	1:1	1:2
structural type	α^t	α^m	α^m	T1	T1	M2
empirical formula	$\text{C}_{44}\text{H}_{36}\text{CoN}_2\text{O}_4$	$\text{C}_{44}\text{H}_{36}\text{N}_2\text{NiO}_4$	$\text{C}_{44}\text{H}_{36}\text{CoN}_2\text{O}_4$	$\text{C}_{50}\text{H}_{42}\text{N}_2\text{NiO}_4$	$\text{C}_{50}\text{H}_{42}\text{CoN}_2\text{O}_4$	$\text{C}_{46}\text{H}_{40}\text{Cl}_4\text{N}_2\text{NiO}_4$
formula unit mass	715.7	715.5	715.7	793.6	793.8	885.3
crystal system	triclinic	monoclinic	monoclinic	triclinic	triclinic	monoclinic
space group	$P\bar{1}$ (no 2)	$P2_1$ (no 4)	$P2_1$ (no 4)	$P\bar{1}$ (no 2)	$P\bar{1}$ (no 2)	$P2_1/c$ (no 14)
a [\AA]	10.590(2)	10.170(2)	10.192(2)	10.282(2)	10.287(2)	17.797(3)
b [\AA]	12.501(2)	20.805(3)	20.864(3)	12.051(2)	12.082(2)	19.808(3)
c [\AA]	15.694(2)	17.622(2)	17.599(2)	16.780(3)	16.802(3)	12.346(2)
α [$^\circ$]	111.42(1)	90	90	95.29(1)	95.05(1)	90
β [$^\circ$]	96.26(1)	101.48(1)	101.40(1)	102.24(1)	101.82(1)	100.83(1)
γ [$^\circ$]	104.96(1)	90	90	92.40(1)	93.07(1)	90
V [\AA^3]	1820.2(5)	3654(1)	3669(1)	2019.2(6)	2030.6(6)	4275(1)
Z	2	4	4	2	2	4
ρ_{calcd} [g cm^{-3}]	1.306	1.301	1.296	1.305	1.298	1.376
reflns for unit cell	all data	all data	all data	all data	all data	all data
$\mu(\text{MoK}\alpha)$ [cm^{-1}]	5.17	5.77	5.13	5.29	4.71	7.49
T [$^\circ\text{C}$]	– 100	– 100	– 100	– 100	– 100	– 100
crystal color	red	yellow-green	red	green-yellow	red	dark yellow
crystal habit	prism	prism	block	prism	block	prism
crystal size [mm]	$0.2 \times 0.2 \times 0.3$	$0.2 \times 0.2 \times 0.5$	$0.4 \times 0.5 \times 0.5$	$0.3 \times 0.3 \times 0.4$	$0.4 \times 0.4 \times 0.4$	$0.2 \times 0.2 \times 0.3$
reflns collected	21 606	43 678	42 433	24 061	23 347	42 221
unique reflns (R_{int})	9349 (0.034)	43 678 (0)	18 905 (0.049)	10 354 (0.019)	10 334 (0.037)	10 789 (0.041)
unique obs reflns ($I > 2\sigma(I)$)	6376	35 036	13 228	7995	7447	6354
refined parameters	463	939	957	517	517	592
$R1/wR2$ (observed data)	0.038/0.083	0.035/0.069	0.044/0.091	0.032/0.079	0.041/0.097	0.042/0.086
$R1/wR2$ (all data)	0.069/0.090	0.052/0.074	0.075/0.099	0.048/0.083	0.064/0.105	0.100/0.100
GOF on F^2	0.981	0.972	0.933	1.013	1.057	0.972
res. density [e \AA^{-3}]	+ 0.27/– 0.38	+ 0.33/– 0.26	+ 0.32/– 0.36	+ 0.25/– 0.29	+ 0.30/– 0.43	+ 0.47/– 0.28
Flack parameter	–	0.405(4)	0.012(8)	–	–	–
CCDC deposition number	150 623	150 624	150 625	150 626	150 627	150 628

Table 1. contd.

Host (M) Guest	Ni 2-Chloropropane	Co 2-Chloropropane	Ni 2-Bromopropane	Co 2-Bromopropane	Ni Chloroform
host:guest ratio	1:2	{1:2}	{1:2}	{1:2}	1:2
structural type	MC	MC	MC	MC	MC
empirical formula	C ₅₀ H ₅₀ Cl ₂ N ₂ NiO ₄	{C ₅₀ H ₅₀ Cl ₂ CoN ₂ O ₄ }	{C ₅₀ H ₅₀ Br ₂ N ₂ NiO ₄ }	{C ₅₀ H ₅₀ Br ₂ CoN ₂ O ₄ }	C ₄₆ H ₃₈ Cl ₆ N ₂ NiO ₄
formula unit mass	872.5	{872.8}	{961.5}	{961.7}	954.2
crystal system	monoclinic	monoclinic	monoclinic	monoclinic	monoclinic
space group or cell type	C2/c (no 15)	C	C	C	C2/c (no 15)
<i>a</i> [Å]	20.164(3)	20.125(6)	20.17(1)	20.108(5)	20.112(3)
<i>b</i> [Å]	19.504(3)	19.554(5)	19.64(1)	19.684(4)	19.567(3)
<i>c</i> [Å]	12.540(2)	12.522(3)	12.585(6)	12.561(3)	12.413(2)
α [°]	90	90	90	90	90
β [°]	116.26(1)	115.49(4)	115.82(7)	114.96(4)	116.46(1)
γ [°]	90	90	90	90	90
<i>V</i> [Å ³]	4423(1)	4448(2)	4487(4)	4507(2)	4373(1)
<i>Z</i>	4	{4}	{4}	{4}	4
ρ_{calcd} [g cm ⁻³]	1.310	{1.303}	{1.423}	{1.417}	1.449
reflins for unit cell	all data	275	88	190	all data
$\mu(\text{MoK}\alpha)$ [cm ⁻¹]	6.06	{5.52}	{22.6}	{22.0}	8.56
<i>T</i> [°C]	-100	-100	-100	-100	-100
crystal color	dark yellow	red	dark yellow	red	dark yellow
crystal habit	prism	prism	prism	prism	block
crystal size [mm]	0.4 × 0.4 × 0.5	0.4 × 0.4 × 0.5	0.3 × 0.3 × 0.4	0.1 × 0.1 × 0.2	0.3 × 0.3 × 0.5
reflins collected	25 507				24 573
unique reflins (<i>R</i> _{int})	5707 (0.027)				5634 (0.034)
unique obs reflins (<i>I</i> > 2σ(<i>I</i>))	4774				4365
refined parameters	286				287
<i>R</i> 1/ <i>wR</i> 2 (observed data)	0.029/0.076				0.037/0.095
<i>R</i> 1/ <i>wR</i> 2 (all data)	0.038/0.080				0.053/0.101
GOF on <i>F</i> ²	1.048				1.058
res. density [e Å ⁻³]	+0.38/-0.40				+0.46/-0.49
CCDC deposition number	150629	150630	150631	150632	150633

Host (M) Guest	Ni Acetone	Co Acetone	Ni Tetrahydrofuran	Ni Nitromethane	Co Nitromethane
host:guest ratio	1:2	{1:2}	1:2	{1:2}	1:2
structural type	MC	MC	MC	MC	MC
empirical formula	C ₅₀ H ₄₈ N ₂ NiO ₆	{C ₅₀ H ₄₈ CoN ₂ O ₆ }	C ₅₂ H ₅₂ N ₂ NiO ₆	{C ₄₆ H ₄₂ N ₄ NiO ₈ }	C ₄₆ H ₄₂ CoN ₄ O ₈
formula unit mass	831.6	{831.8}	859.7	{837.6}	837.8
crystal system	monoclinic	monoclinic	monoclinic	monoclinic	monoclinic
space group or cell type	C2/c (no 15)	C	C2/c (no 15)	C	C2/c (no 15)
<i>a</i> [Å]	19.994(3)	19.942(8)	20.190(3)	19.373(6)	19.199(3)
<i>b</i> [Å]	19.649(3)	19.720(9)	19.471(3)	19.799(6)	19.873(4)
<i>c</i> [Å]	12.687(2)	12.655(4)	13.054(2)	12.633(4)	12.537(2)
α [°]	90	90	90	90	90
β [°]	119.01(1)	118.58(4)	118.75(1)	118.43(6)	116.79(1)
γ [°]	90	90	90	90	90
<i>V</i> [Å ³]	4359(1)	4370(3)	4499(1)	4261(2)	4270(1)
<i>Z</i>	4	{4}	4	{4}	4
ρ_{calcd} [g cm ⁻³]	1.267	{1.264}	1.269	{1.306}	1.303
reflins for unit cell	all data	98	all data	177	all data
$\mu(\text{MoK}\alpha)$ [cm ⁻¹]	4.96	{4.44}	4.83	{5.13}	4.59
<i>T</i> [°C]	-100	-100	-100	-100	-100
crystal color	dark yellow	red	dark yellow	dark yellow	red
crystal habit	block	block	prism	prism	prism
crystal size [mm]	0.2 × 0.3 × 0.3	0.2 × 0.2 × 0.2	0.3 × 0.3 × 0.4	0.2 × 0.2 × 0.4	0.2 × 0.3 × 0.5
reflins collected	25 579		26 306		24 424
unique reflins (<i>R</i> _{int})	5629 (0.039)		5787 (0.035)		5491 (0.043)
unique obs reflins (<i>I</i> > 2σ(<i>I</i>))	3987		4199		3804
refined parameters	328		313		307
<i>R</i> 1/ <i>wR</i> 2 (observed data)	0.038/0.093		0.038/0.108		0.045/0.116
<i>R</i> 1/ <i>wR</i> 2 (all data)	0.064/0.100		0.060/0.116		0.074/0.125
GOF on <i>F</i> ²	0.989		1.045		1.022
res. density [e Å ⁻³]	+0.41/-0.36		+0.41/-0.32		+0.44/-0.26
CCDC deposition number	150634	150635	150636	150637	150638

The above approach uses several assumptions, the most important ones being that the sample studied contains only the three phases at each point in time, that no amorphous intermediates form in significant quantities, that the presence of other phases does not change peak intensities for a given phase significantly, and that the intensity of peaks for the clathrate phase does not change significantly for different guests. We believe that the systematic errors caused by the use of these assumptions do not exceed random errors that may be as high as 7–8%.

Results and Discussion

Propensity for clathrate formation of the title complexes in monoclinic form: Table 2 summarizes results for clathrate formation of the $[\text{Ni}(4\text{-ViPy})_2(\text{DBM})_2]$ host complex in its monoclinic, α^m form. The complex reacts with methylene chloride, chloroform, 2-chloro- and 2-bromopropanes, acetone, tetrahydrofuran and nitromethane to give 1:2 (host: guest) inclusions, whereas with benzene, the 1:1 inclusion is observed. Data on inclusions with carbon tetrachloride (1:2) and chlorobenzene (1:1) reported earlier^[2] are also listed in Table 2. No reaction was observed with hexane, the alcohols listed, 2,2-dimethoxypropane and ethyl acetate. Almost in all cases, the final products after crystallization (from neat guest liquid) and after isopiestic experiments (interaction of solid host with guest vapors) coincided. The results of single-crystal X-ray experiments allow the classification of the resulting inclusions into five structural types, and provide structural guest per host stoichiometries. In cases where structures were completely solved, the refined guest to host ratios are very nearly ideal, which suggests full cavity occupancy under the experimental conditions used. Isopiestic measurements followed by powder X-ray analysis provide independent confirmation of compositions and structural types of the resulting inclusions and give evidence that the reactions for all the

bulky samples proceed completely to the unique final products.

Table 3 shows results for clathrate formation by $\alpha^m\text{-}[\text{Co}(4\text{-ViPy})_2(\text{DBM})_2]$. With some guests, reaction products similar to those for the Ni-complex formed. Some of the solvents, which do not react as guests, still are active by catalyzing the transformation of the monoclinic form to the triclinic form of the Co-host. With some solvents (especially chloroform and nitromethane) the formation of inclusion compounds was observed in the first few hours (from the mass increase and powder XRD tests) but these disappeared later to give the triclinic guest-free polymorph. From Table 3, another feature to be noted is that isopiestic and crystallization products are different in some cases, suggesting sensitivity of the processes to experimental conditions. This may mean that there are small energy differences between the two potential products and that there are kinetic problems associated with the heterogeneous interaction in isopiestic experiments. Thus, unlike the isopiestic method, direct crystallization results in inclusion crystals with carbon tetrachloride, nitromethane and chlorobenzene. On the other hand, the high reaction affinity of the vinyl group adversely affects crystallization results in the case of methylene chloride or tetrahydrofuran, suggesting that the isopiestic method is more appropriate when these solvents are used.

Clathration ability vs polymorphism of the title complexes

Isolated polymorphic types: Two guest-free polymorphs of the Ni-complex and three of the Co-complex were isolated. Both complexes have α^m - and β forms, which are isostructural in pairs while the Co-complex possesses also a third, triclinic α^t form (Figure 1).

The stability of the observed polymorphs decreases in the sequence $\alpha^m > \beta$ for Ni-complex and $\alpha^t > \alpha^m > \beta$ for the Co-complex. Qualitatively, the corresponding Ni polymorphs are more stable than the Co-ones. This is consistent with stronger coordination by Ni^{II} compared with Co^{II} .^[11] The control over stability of inclusion compounds upon replacing the metal center in the host without changing the crystal structure is one of the great advantages of metal–complex hosts. The regular influence of coordination bond strength on macroproperties of metal–complex hosts and their clathrates was established unambiguously in several earlier isomorphous series.^[12] The observed polymorphism indicates that there are problems for the complex molecules to create an effective structure providing both favorable molecular conformations and ef-

Table 2. Products of the interaction of the α^m form of $[\text{Ni}(4\text{-ViPy})_2(\text{DBM})_2]$ host complex (H) with guest solvents (G).

Guest solvent (G)	Isopiestic experiment (interaction with solvent vapor)		Crystallization from neat solvent		
	G:H (from mass increase)	Structure-type (powder X-ray experiment)	G:H (single-crystal X-ray experiment)	Structural type	Assigned reaction product
methylene chloride	2.00(1)	M2 or MC	1.99(3)	M2	H*2G
chloroform	2.01(1)	M2 or MC	1.946(5)	MC	H*2G
carbon tetrachloride	too slow	–	1.96(4)	T2	H*2G
2-chloropropane	1.93(1)	M2 or MC	1.99(1)	MC	H*2G
2-bromopropane	1.99(1)	M2 or MC	–	MC	H*2G
<i>n</i> -hexane	little ^[a]	α^m (host)	–	α^m (host)	no reaction
methanol	little ^[a]	α^m (host)	–	α^m (host)	no reaction
ethanol	little ^[a]	α^m (host)	–	α^m (host)	no reaction
<i>n</i> -propanol	little ^[a]	α^m (host)	–	α^m (host)	no reaction
isopropanol	little ^[a]	α^m (host)	–	no crystals	no reaction
acetone	2.02(2)	M2 or MC	1.98(1)	MC	H*2G
tetrahydrofuran	2.006(6)	M2 or MC	2.06(2)	MC	H*2G
2,2-dimethoxypropane	little ^[a]	α^m (host)	–	α^m (host)	no reaction
ethyl acetate	little ^[a]	α^m (host)	–	α^m (host)	no reaction
nitromethane	2.02(1)	M2 or MC	–	MC	H*2G
benzene	1.03(1)	T1	1.013(2)	T1	H*G
chlorobenzene	too slow	–	1.00(1)	M1	H*G

[a] In this and subsequent tables “little” means “within 0.01–0.06”.

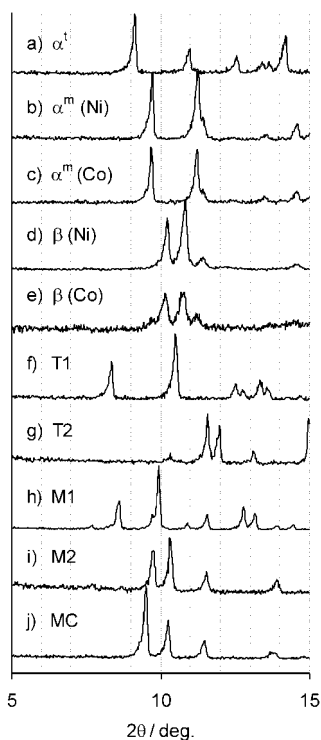


Figure 1. Selected powder diffractograms ($\text{CoK}\alpha$, $\lambda = 1.7902 \text{ \AA}$) representing three polymorphic host and five clathrate structural types: a) $[\text{Co}(4\text{-ViPy})_2(\text{DBM})_2]$, α^1 polymorph; b) $[\text{Ni}(4\text{-ViPy})_2(\text{DBM})_2]$, α^m polymorph; c) $[\text{Co}(4\text{-ViPy})_2(\text{DBM})_2]$, α^m polymorph; d) $[\text{Ni}(4\text{-ViPy})_2(\text{DBM})_2]$, β polymorph (prepared by decomposition of clathrate with methylene chloride); e) $[\text{Co}(4\text{-ViPy})_2(\text{DBM})_2]$, β polymorph (prepared by decomposition of clathrate with methylene chloride); f) $[\text{Ni}(4\text{-ViPy})_2(\text{DBM})_2] \cdot (\text{C}_6\text{H}_6)$, T1-type; g) $[\text{Ni}(4\text{-ViPy})_2(\text{DBM})_2] \cdot 2(\text{CCl}_4)$, T2-type; h) $[\text{Ni}(4\text{-ViPy})_2(\text{DBM})_2] \cdot (\text{C}_6\text{H}_5\text{Cl})$, M1-type; i) $[\text{Ni}(4\text{-ViPy})_2(\text{DBM})_2] \cdot 2(\text{CH}_2\text{Cl}_2)$, M2-type; j) $[\text{Ni}(4\text{-ViPy})_2(\text{DBM})_2] \cdot 2(\text{CH}_3\text{COCH}_3)$, MC-type.

fective packing. Apparently, this property is responsible for the versatility of the title complexes and their analogues to form inclusion compounds. In a broad sense, the inclusion compounds are often considered to be polymorphic modifi-

cations of the host component, which are stable only in the presence of a templating guest.^[13] From this viewpoint, conventional polymorphism and the affinity to include would seem to be closely related to each other, and this relationship is obvious in the many cases where they are found together such as in the current work.^[14]

Forms of the Ni-complex and reactivity of the β polymorph:

The monoclinic (α^m) form of the Ni-complex is a stable polymorph; it forms during the course of synthesis and crystallizes from solvents which do not react as guests (Tables 2, 4). The majority of inclusions shown in Table 2 transform to the stable form upon decomposition.

The metastable β form forms reproducibly upon decomposition of inclusions with methylene chloride and acetone, and sometimes of inclusions with nitromethane. It is stable in air at least for several months, but heating induces its collapse to the α^m form; alternatively, solvent vapors catalyze this transformation very well (Table 4). Possibly, all inclusions of the MC-type should be able to give the β form upon decomposition, but vapors of the released guest catalyze the formation of the α^m form. Inclusions with methylene chloride and acetone decompose markedly faster because of the greater mobility of the guest species, as the host system apparently has no time to reassemble into the stable modification. At the same time, powder X-ray diffraction analysis indicates that the β form differs structurally from the inclusions studied and apparently does not possess available pore space. This conclusion follows from kinetic experiments (see below) showing that the powder diffractogram does not change continuously during formation of inclusion compounds from the β polymorph, and peaks of both phases may be observed simultaneously.

A quantitative comparison of the relative stability of the α and β polymorphs follows from DSC experiments (Figure 2). The α form shows no thermal effects upon heating up to a

Table 3. Products of the interaction of the α^m form of the $[\text{Co}(4\text{-ViPy})_2(\text{DBM})_2]$ host complex (H) with guest solvents (G).

Guest solvent (G)	Isopiestic experiment (interaction with solvent vapor)		Crystallization from neat solvent		Assigned reaction product
	G:H (from mass increase)	Structural type (powder X-ray experiment)	G:H	Structural type (single-crystal X-ray experiment)	
methylene chloride	2.03(2)	M2 or MC		no crystals	H*2G (isopiestic.)
chloroform	irreproducible	α^1 (host)+mix	–	α^1 (host)	α^1 -H (crystal.)
carbon tetrachloride	little	$\alpha^m + \alpha^1$ (host)	1.94(4)	T2	H*2G (crystal.)
2-chloropropane	2.01(1)	M2 or MC		MC	H*2G
2-bromopropane	1.90(1)	M2 or MC		MC	H*2G
n-hexane	little	α^m (host)		no crystals	no reaction
methanol	little	α^m (host)	–	α^1 (host)	α^1 -H (crystal.)
ethanol	little	α^m (host)	–	α^1 (host)	α^1 -H (crystal.)
n-propanol	little	α^m (host)		no crystals	no reaction
isopropanol	little	α^m (host)		no crystals	no reaction
acetone	2.02(1)	M2 or MC		MC	H*2G
tetrahydrofuran	2.02(1)	M2 or MC		no crystals	H*2G (isopiestic.)
2,2-dimethoxypropane	little	α^m (host)	–	α^1 (host)	α^1 -H (crystal.)
ethyl acetate	little	α^1 (host)	–	α^1 (host)	α^1 -H
nitromethane	irreproducible	α^1 (host)	1.99(2)	MC	H*2G (crystal.)
benzene	1.022(7)	T1	1.012(3)	T1	H*G
chlorobenzene	little	α^1 (host)	0.99(1)	M1	H*G (crystal.)

Table 4. Interaction of β form of $[\text{Ni}(\text{4-ViPy})_2(\text{DBM})_2]$ host complex (H) with guest solvents (G), the isopiestic and X-ray powder experiments results.^[a]

Guest solvent (G)	G:H	Structural type	Assigned reaction product
<i>n</i> -pentane	1.03(1)	M2 or MC	H*G
isopentane	little	α^m (host)	α^m -H
cyclopentane	little	α^m (host)	α^m -H
<i>n</i> -hexane	1.00(1)	M2 or MC	H*G
neohexane (2,2-dimethylbutane)	little	α^m (host)	α^m -H
cyclohexane	little	α^m (host)	α^m -H
<i>n</i> -heptane	1.00(1)	M2 or MC	H*G
<i>n</i> -octane	little	α^m (host)	α^m -H
<i>n</i> -nonane	little	α^m (host)	α^m -H
<i>n</i> -decane	little	α^m (host)	α^m -H
1-chloropentane	1.08(3)	M2 or MC	H*G
1,1-dichloroethane	2.03(2)	M2 or MC	H*2G
1,2-dichloroethane	irreproducible	α^m (host)	α^m -H
1,2-dichloropropane	irreproducible	α^m (host)	α^m -H
3-chloropropene	little	α^m (host)	α^m -H
2,2-dichloro-1,1,1-trifluoroethane	little	α^m (host)	α^m -H
methanol	little	α^m (host)	α^m -H
ethanol	little	α^m (host)	α^m -H
<i>n</i> -propanol	little	α^m (host)	α^m -H
isopropanol	little	α^m (host)	α^m -H
<i>n</i> -butanol	little	α^m (host)	α^m -H
methyl <i>tert</i> -butyl ether	little	α^m (host)	α^m -H
dimethoxymethane	little	α^m (host)	α^m -H
1,2-dimethoxyethane	1.18(2)	M2 or MC	H*1.2G
2,2-dimethoxypropane	little	α^m (host)	α^m -H
2-butanone	little	α^m (host)	α^m -H
2-pentanone	1.16(3)	M2 or MC	H*1.2G
methyl acetate	little	α^m (host)	α^m -H
ethyl acetate	1.09(1)	M2 or MC	H*1.1G
diethyl carbonate	≈ 1	M2 or MC	H*G

[a] With methylene chloride, chloroform, 2-chloropropane, 2-bromopropane, acetone, tetrahydrofuran, nitromethane and benzene the β form gives the same clathrates as α - $[\text{Ni}(\text{4-ViPy})_2(\text{DBM})_2]$ (Table 2).

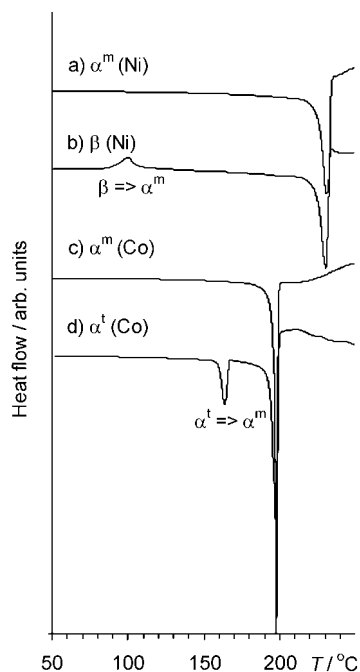


Figure 2. DSC thermograms (heat flow vs temperature; heating rate 5° per min) of host polymorphs: a) $[\text{Ni}(\text{4-ViPy})_2(\text{DBM})_2]$, α^m polymorph (5.46 mg); b) $[\text{Ni}(\text{4-ViPy})_2(\text{DBM})_2]$, β polymorph (5.47 mg); c) $[\text{Co}(\text{4-ViPy})_2(\text{DBM})_2]$, α^m polymorph (4.78 mg); d) $[\text{Co}(\text{4-ViPy})_2(\text{DBM})_2]$, α^t polymorph (6.10 mg). The polymorphic transformations are assigned on the thermograms b) (*exo* effect at 70°C) and d) (*endo* effect at 160°C).

strong endotherm at 226(1)°C, suggesting melting of this phase. The β form shows an exotherm at 90(1)°C, with the rest of the thermogram being identical to that for the α form. The exotherm indicates an irreversible, thermally induced, change of the metastable β form to the stable α form. Assuming that all of the process occurs in the 80–130° temperature range, the β to α transformational enthalpy is $-11.3(2)$ kJ mol⁻¹ at this temperature.

The propensity of the β form for clathrate formation is remarkably high, as evident both from the inclusion reaction rates and from the range of guests that may be enclathrated. The β form gives the same clathrates with the guests as the α^m form, but the reactions occur faster. Moreover, the β form enclathrates a number of guests to which the α^m form is indifferent: *n*-pentane, *n*-hexane, *n*-heptane, 1-chloropentane, 1,2-dimethoxyethane, 2-pentanone, and ethyl acetate. Actually, as partly illustrated by Table 4, the

β form reacts with all volatile organics to give the host α^m form unless inclusion compounds are formed.

The higher clathratogenic potential of the β polymorph may be understood in light of considerations reported elsewhere.^[15, 16] According to this scheme, a clathrate formation process may be carried out conceptually by following several simple steps. One of these, involving the host only, is energetically unfavorable but unavoidable; it usually can be split into two terms: the polymorph transformation of the non-clathrate α form to the empty clathrate β form ($\Delta H_{\alpha-\beta}$) and dilation of the β form that occurs on absorption of the guest ($\Delta H_{\beta-\beta^*}$). The utilization of the β form, even if it does not possess permanent porosity, may thus facilitate the clathrate formation process. The $\Delta H_{\alpha-\beta} = 11.3(2)$ kJ mol⁻¹ is rather significant and may be compared with 3.5(1) kJ mol⁻¹ for the $\alpha \rightarrow \beta$ transformation of the $[\text{Ni}(\text{4-MePy})_4(\text{NCS})_2]$ host^[16] and 0.5(1) kJ mol⁻¹ for hydroquinone.^[17]

We propose that the β polymorph is a state of the host able to transform instantly into the clathrate. This state of the host component was referred to as the “apohost”.^[18] The structural rearrangement of molecules on going from the “apohost phase” to the clathrate phase is simple, as it does not require breaking of bonds, high-energy movement of host molecules, and so on, thus maintaining a low activation barrier of the process. The “apohost” is thus a “compressed” empty clathrate form showing zeolitic properties in spite of the

absence of permanent porosity. One of first “organic zeolite” analogues studied,^[19, 20] β -[Ni(4-MePy)₄(NCS)₂],^[21] revealed porosity in the complete absence of included guest species. At the same time, this robust host framework reveals a remarkable flexibility by expanding its structure by up to 10% to include guest molecules.^[19] The realization of “flexible zeolite mimics” is thus demonstrated in our work: The empty host phase doesn’t have porosity at all but acquires it instantly upon the presence of the guest, thus behaving as if it were permanently microporous. In spite of differences in the powder diffractograms, the generic relationship between β -[Ni(4-ViPy)₂(DBM)₂] and the M2 or MC clathrate types is evident as the former arises from the clathrate types upon fast release of the guest components.

Kinetic experiments provide further support of this relationship. Interaction of the β form with *n*-pentane is an inclusion process that occurs without an observable induction period (Figure 3a). At the same time, relaxation of the β form to the α form (Figure 3b) seems to be a process requiring a more serious structural reconfiguration.

The kinetic curves (Figure 3) reveal other interesting features as well. Reacting the β polymorph with an atmosphere of three different pentane hydrocarbons gives rise to quite different types of behavior. With *n*-pentane, an inclusion compound forms, whereas cyclopentane does not support an inclusion structure thus catalyzing the collapse to the stable α polymorph, and isopentane forms an inclusion compound as an intermediate product which then disappears, yielding the α polymorph. The whole process with isopentane is dramatically slower in spite of the greatest volatility, and thus the highest concentration, of isopentane as compared to the other pentanes. These results, and data listed in Table 4, illustrate the selectivity the β form shows to certain isomers or homologues. The observed preferences are understandable upon considering the crystal packing inherent in the M2 and MC types, as discussed below.

Forms of Co-complex: The Co-complex forms three guest-free polymorphs, two of which are isostructural with the corresponding Ni-forms. The monoclinic α^m form precipitates during the synthesis and is stable in air but transforms slowly to the thermodynamically stable triclinic α^t form if left in ethanol. Also, non-included solvents, as seen from Table 5, catalyze this transformation. Subjected to DSC measurements (Figure 2), the α^m form shows no change until melting at 193 °C, while the α^t form shows an endotherm of 15.9(1) kJ mol⁻¹ at 160 °C followed by melting with the same parameters as for the α^m form. These observations show that the α^m form is actually a high-temperature polymorph of the complex stable in the 164–193 °C range. The 15.9(1) kJ mol⁻¹ energy difference between the two α polymorphs explains their different propensities for clathrate formation. As evident from comparing Tables 3 and 5, the α^t form shows a significantly lower clathrate formation ability, forming inclusions only with methylene chloride, acetone and tetrahydrofuran of the seventeen guests tested. The β form of the Co-complex is extremely unstable, as it appears upon fast decomposition of the clathrate with methylene chloride (Figure 1e) but spontaneously transforms to the more stable polymorphs.

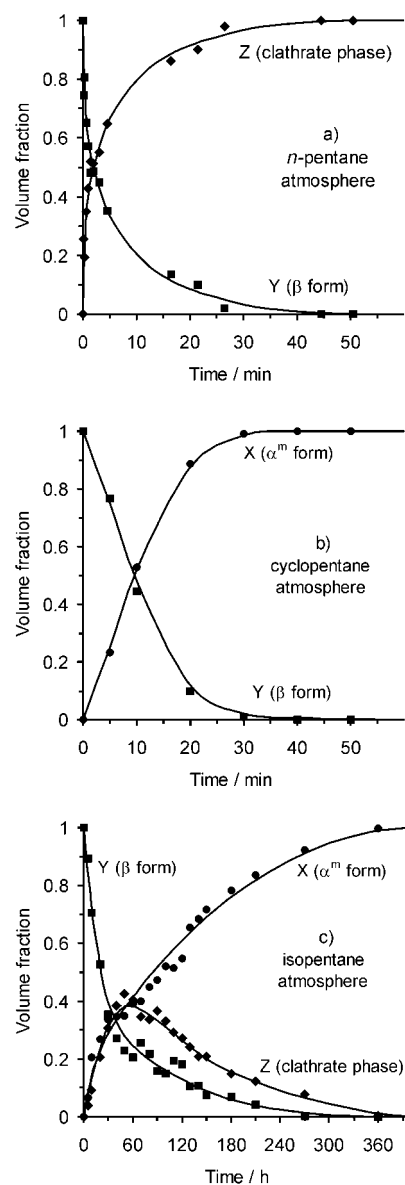


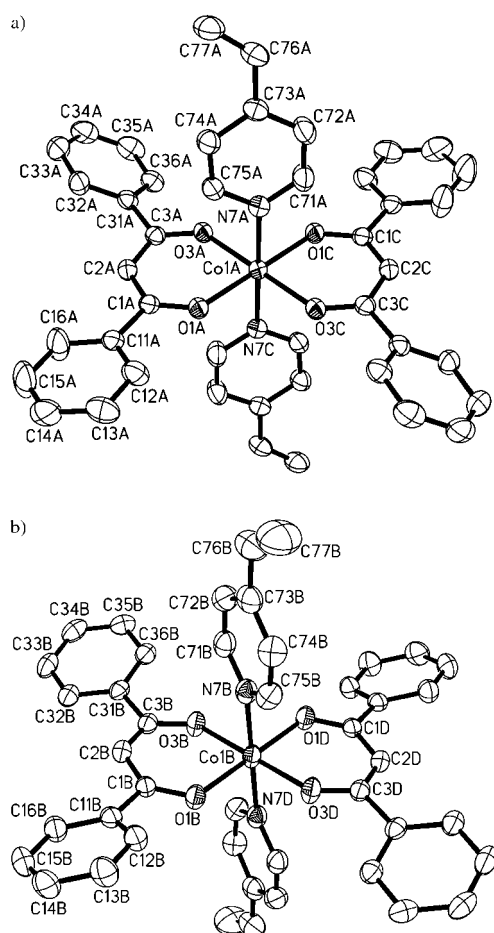
Figure 3. Kinetic curves showing the volume fractions of the solid α^m -form X (circles), β -form Y (squares) of the [Ni(4-ViPy)₂(DBM)₂] complex, and the clathrate phase Z (diamonds) vs time. All experiments start with pure β form (Y=1). Reaction gases (at 1 atm): *n*-pentane a), cyclopentane b), isopentane c).

Structural characteristics of host and clathrate types

Structure and conformations of the host molecule: Eleven (three host and eight clathrate) structures belonging to seven structural types were completely solved in this and in previous^[2] works. These structures comprise seven variations of the [Co(4-ViPy)₂(DBM)₂] molecule and ten of the [Ni(4-ViPy)₂(DBM)₂] molecule. In all structures the molecules appear as *trans* isomers, with the metal(II) center chelated by two DBM units in the equatorial plane and two vinylpyridine ligands coordinated axially, as exemplified by Figure 4. The M–O distance varies within 2.016–2.056 Å with an average value of 2.039(2) Å (24 independent bonds) for M = Co and within 1.999–2.042 Å with an average of 2.022(2) Å (30 bonds) for Ni. The M–N bonds are longer, varying from

Table 5. Interaction of α' form of $[\text{Co}(4\text{-ViPy})_2(\text{DBM})_2]$ host complex (H) with guest solvents (G), the isopiestic experiment data.

Guest solvent (G)	G:H (from mass increase)	Structural type (powder X-ray experiment)	Assigned reaction product
methylene chloride	1.99(1)	M2 or MC	H*2G
chloroform	little	α' (host)	no reaction
carbon tetrachloride	little	α' (host)	no or slow reaction
2-chloropropane	little	α' (host)	no or slow reaction
2-bromopropane	little	α' (host)	no or slow reaction
<i>n</i> -hexane	little	α' (host)	no reaction
methanol	little	α' (host)	no reaction
ethanol	little	α' (host)	no reaction
<i>n</i> -propanol	little	α' (host)	no reaction
isopropanol	little	α' (host)	no reaction
acetone	2.00(1)	M2 or MC	H*2G
tetrahydrofuran	2.02(3)	M2 or MC	H*2G
2,2-dimethoxypropane	little	α' (host)	no reaction
ethyl acetate	little	α' (host)	no reaction
nitromethane	little	α' (host)	no reaction
benzene	little	α' (host)	no reaction
chlorobenzene	little	α' (host)	no or slow reaction

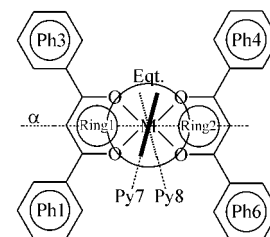
Figure 4. Structure of the $[\text{Co}(4\text{-ViPy})_2(\text{DBM})_2]$ molecules as they are found in the stable α' polymorph of the complex: a) A-molecule; b) B-molecule. H-atoms are omitted; ellipsoids are drawn at 50% probability level; C- and D-labeled atoms are generated through centrosymmetry.

2.157–2.206 Å with an average of 2.181(5) Å (12 bonds) for M = Co and 2.091–2.117 with an average of 2.109(3) Å (15 bonds) for Ni. The difference between the length of M–O and

M–N bonds may be accounted for both by the negative charge and the chelating coordination mode of DBM ligand. In the clathrate structures the average M–O distance is slightly longer, while the M–N distance is slightly shorter. For example, the average Co–O distances are 2.042(2) Å (12 bonds) and 2.035(3) Å (12 bonds) for clathrate and guest-free structures, respectively, while the corresponding Co–N distances are 2.171(3) Å (six bonds) and 2.191(7) Å (six bonds). On the whole, a reverse correlation is observed between changes in equatorial and axial bonds, a phenomenon reviewed earlier^[22] and reported

for the *trans*- $[\text{Ni}(4\text{-MePy})_4(\text{NCS})_2]$ host molecule (statistics from eleven structures^[23]). The coordination angles rarely deviate from the ideal by more than 3°. The deviations may be explained in part by restrictions from the fixed geometry of the pseudo-aromatic chelate rings; for example, average values of the O–M–O angles included in the chelate ring are 89.3(2)° (12 independent angles) for M = Co but 91.4(1)° (15 angles) for Ni. In general, statistical analysis of coordination polyhedra does not reveal drastic differences between molecules in guest-free and clathrate phases. This means that the improvement of the complex molecular geometry is not a driving force for clathration with the title hosts, unlike with some tetrapyrroline Werner hosts reported earlier.^[24] The profit of clathrate formation in our case lies in the provision of better packing.

Conformational features are summarized in Table 6. As the conformations for molecules in isostructural phases do not differ qualitatively, only average values for each structural type are given. In most cases the molecule adopts centrosymmetry. Pseudo-aromatic chelate rings which reveal planarity (almost always within 0.1 Å) are in one plane, and in this case additional interactions are possible between their delocalized π systems through empty orbitals on the metal center. In the α^m and M1 types, however, the bis-chelate fragment is bent significantly, up to 25°. Though peripheral phenyl rings are not able to turn in the equatorial plane (because of repulsion between the *ortho* hydrogens with the hydrogen attached to the middle carbon of DBM) they still show an unequivocal tendency to do so. As one can see from Table 6, the dihedral angle between phenyls and the equatorial plane in 84% of the cases does not exceed 30° (see also Scheme 2). Vinylpyridine ligands (which are always essentially planar) are attached



Scheme 2. Descriptors for Table 6.

approximately at right angles to the equatorial plane; in centrosymmetric structures two vinylpyridine ligands are in the same plane and vinyl groups are directed oppositely. This also assumes a possibility for the two vinylpyridine aromatic systems to interact. Almost in all conformations, vinylpyridine rings are close to a plane that divides the metal bis-chelate fragment into two parts. Figure 4a exemplifies the only exception found with vinylpyridines turned along bis-chelate.

The above analysis shows that the *trans*-[M(4-ViPy)₂(DBM)₂] molecule possesses a certain flexibility but shows an unequivocal tendency to a preferred, centrosymmetric type of conformation. The conformation would have planar bis-chelate fragments with phenyl rings slightly deviating from the plane, and vinylpyridine ligands coordinated axially and located in the plane dividing the bis-chelate fragment into two parts. The conformation is likely controlled not only by steric intramolecular interactions but also by the interacting local aromatic systems connected by a single bond or the metal center. Nevertheless, certain, though limited, flexibility makes it possible for the molecule to adopt different geometries, allowing the creation of a number of dense and porous frameworks filled with different guest components.

Main packing motifs: All of the phases that the title hosts form are controlled by van der Waals forces.^[25] This results in a variety of crystal structures that are different crystallographically and topologically. The absence of directed chemical or specific interactions between molecules make the description of “host frameworks” rather arbitrary. Very small changes in the conformations or mutual orientations of host molecules may result in a dramatic change in size, shape and dimensionality of cavity space available for the guest. Therefore, before describing individual types, here we discuss the structural motifs observable in most phases.

The *trans*-[M(4-ViPy)₂(NCS)₂] molecule in its usual conformation, as shown on Figure 4b, has four shallow pockets

each located between the vinylpyridine and DBM fragments (cf. the same Figure, a, where such pockets disappear due to a rotating vinylpyridine). These pockets are filled upon packing either with aromatic parts of neighboring host molecules, or with guest molecules. Earlier, this viewpoint allowed us to explain the clathration ability and stoichiometry of clathrates of the *trans*-[NiPy₂(DBM)₂] complex. Introducing a vinyl-substituted pyridine elongates the pocket and thus enhances the clathration affinity of the molecule.

Figure 5 shows two host molecules mutually expanding the size of their pockets as these are filled by vinylpyridine moieties. Note that the molecules approach each other in such a way that they form stacking vinylpyridines and the dihedral angle between their equatorial planes is less than 90°. Each

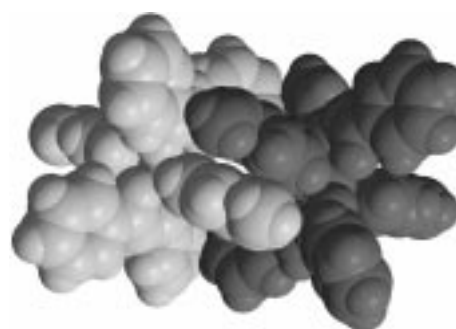


Figure 5. Two adjacent molecules in the crystal structure of α^m -[Co-(4-ViPy)₂(DBM)₂] shown according to their van der Waals size. The molecules are self-included, as each molecule slips its vinylpyridine moiety into pocket of another molecule. For clarity, molecule A is darkened and molecule B is lightened.

molecule has two neighbors on both sides of an equatorial plane, the motif thus consisting of endless chains as exemplified by Figure 6. These chains were found in most structures; moreover, the parameters of the chains are very similar in

Table 6. Averaged conformational characteristics for the *trans*-[M(4-ViPy)₂(DBM)₂] molecule found in different structures.

Structural type	Point symmetry	Ring 1 – Ring 2	Eq. - Ph1	Eq. - Ph3	Dihedral angles [°] ^[a]						Vinyl groups
					Eq. - Ph4	Eq. - Ph6	Eq. - Py7	Eq. - Py8	α -Py7	α -Py8	
α^t (one structure), molecule A:	–1	0	+7	+26	–7	–26	83	83	+13	–13	opposite
molecule B:	–1	0	+22	–18	–22	+18	86	86	+63	–63	opposite
α^m (two structures), molecule A:	1	7	+18	–52	–27	+41	72	90	+87	+66	opposite or disordered
molecule B:	1	16	+34	–16	–24	+26	83	88	+89	–85	disordered
T1 (two structures), molecule A:	–1	0	+8	+41	–8	–41	83	83	+87	–87	opposite
molecule B:	–1	0	+30	–30	–30	+30	89	89	+72	–72	opposite
T2 (two structures): M1 (two structures): M2 (one structure) molecule A:	–1	0	+22	+19	–22	–19	83	83	+75	–75	opposite
molecule B:	1	25	+22	+36	+15	+46	85	84	+69	–86	opposite
molecule A:	–1	0	+29	–20	–29	+20	87	87	+84	–84	opposite
molecule B:	–1	0	+24	–29	–24	+29	86	86	+83	–83	disordered
MC (five structures):	–1	0	+23	–28	–23	+28	86	86	+86	–86	opposite or disordered

[a] Least-squares planes are designated as shown on the Scheme 2. For example, the planes for the molecule shown in Figure 4a are as follows: Ring 1 (Co1A, O1A, C1A, C2A, C3A, O3A); Ring 2 (Co1A, O1C, C1C, C2C, C3C, O3C); Eq. (Co1A, O1A, O3A, O1C, O3C); Ph1 (C11A–C16A); Ph3 (C31A–C36A); Ph4 (C11C–C16C); Ph6 (C31C–C36C); α (Co1A, C2A, C2C, N7A, N7C); Py7 (N7A, C71A–C75); Py8 (N7C, C71C–C75C).

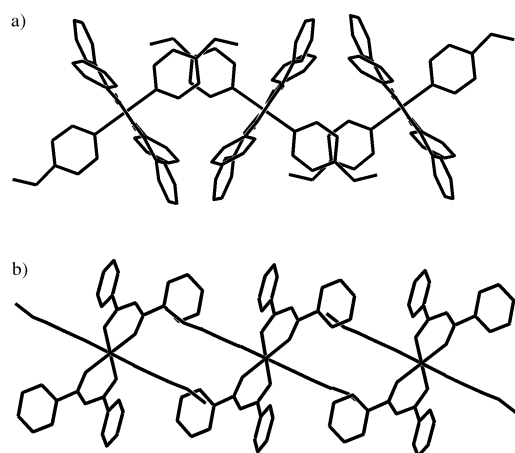


Figure 6. Fragment of the chain of host molecules in the crystal structure of $[\text{Ni}(4\text{-ViPy})_2(\text{DBM})_2] \cdot 2(\text{CH}_3\text{COCH}_3)$ (MC type): a) perpendicular to the stacking vinylpyridines; b) parallel to the stacking vinylpyridines.

different structures (Table 7) and always are aligned parallel to each other. In some cases they consist of crystallographically distinct alternating molecules. The distance between metal centers varies from 8.2–9.4 Å, the distance between stacking vinylpyridine rings from 3.4–3.8 Å with the angle not exceeding 15°, and with the angle between equatorial planes of 64–74°. Note that variations between different structural types do not significantly exceed those from within the same type. This chain motif thus is not only encountered in different phases but also is rather insensitive to the phase type. The reason for this is that this motif provides very effective one-dimensional packing. At the same time, it seems to be difficult to pack the chains in three-dimensional space. The α^m host type shows significant distortions of the chain without guests present. Compared to the clathrate types, the chain in the α^m phase has maximum (11° and 15°) angles between stacking vinylpyridine rings, a minimum angle (64°) between equatorial planes, and alternating shortened (8.2 Å) and elongated (9.4 Å) M–M distances. In clathrate types the packing of chains is assisted by guest species.

As the host molecule has four pockets, and only two may be filled with vinylpyridine moieties of neighboring hosts, the other two pockets are available to guests. Figure 7a shows the filling of two pockets with two methylene chloride molecules. The host:guest stoichiometry should be 1:2 in such a case, and this ratio is indeed observed for most inclusions. Two pockets from two adjacent host molecules may form a larger cavity; Figure 7b exemplifies this option by including a benzene

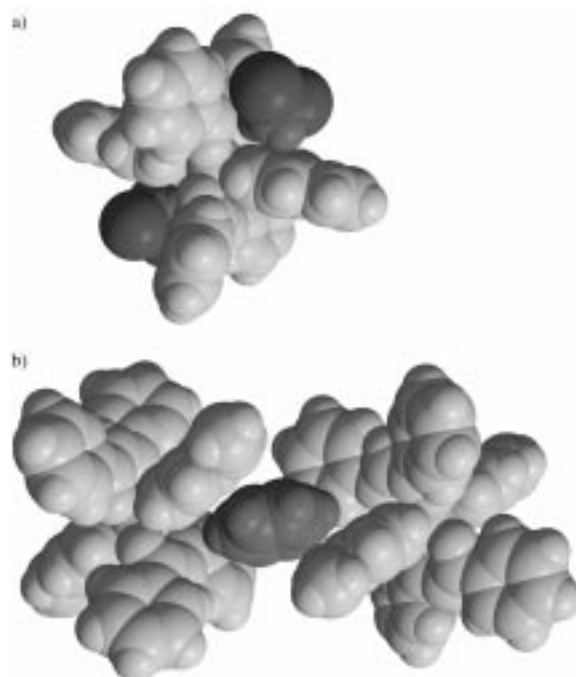


Figure 7. Typical host-guest packing fragments: a) two guest molecules filling the pockets on opposite sides of the host molecule in $[\text{Ni}(4\text{-ViPy})_2(\text{DBM})_2] \cdot 2(\text{CH}_2\text{Cl}_2)$ (M2-type); b) a guest molecule occupying the large cavity formed by two adjoining pockets from adjacent molecules (molecule A on the left and B on the right) in $[\text{Ni}(4\text{-ViPy})_2(\text{DBM})_2] \cdot (\text{C}_6\text{H}_6)$ (T1 type). All molecules are shown at their van der Waals size; guest molecules are drawn darker for clarity.

molecule between two hosts, thus resulting in a 1:1 stoichiometry. In T2-type inclusions described earlier^[2] all pockets are involved in the inclusion of carbon tetrachloride guest molecules; four pockets from four host molecules (located in the corners of the unit cell) form one very large cavity accommodating two guest molecules, resulting in a stoichiometry of 1:2.

α^t and α^m host types: The α^t type forms only for the Co complex. It is triclinic, with two centrosymmetric molecules per unit cell. They are crystallographically different (A and B here after, see Figure 4). The A-molecule has an unusual shape as the vinylpyridine ligand is turned along the bis-chelate unit. The B-molecule resembles more closely a regular conformation. There are chains of alternating A and B molecules stretching parallel in a diagonal direction between the *a* and *c* axes (Figure 8). These chains are, however,

Table 7. Parameters of one-dimensional packing of *trans*- $[\text{M}(4\text{-ViPy})_2(\text{DBM})_2]$ molecules in studied types.

Structural type	α^m	T1	M1	M2	MC
number of examined structures	2	2	2	1	5
direction of chains	along <i>c</i>	diagonally between <i>a</i> and <i>c</i>	along <i>c</i>	along <i>a</i>	parallel to direction between <i>a</i> and <i>c</i>
sequence of molecules	ABAB	ABAB	AAAA	ABAB	AAAA
M...M distance	8.2 and 9.4 Å	8.9 Å	8.8 Å	8.9 Å	8.8–9.2 Å
dihedral angle ^[a]	11 and 15°	9°	7°	8°	1–6°
distance between these rings	3.4–3.8 Å	3.4–3.8 Å	3.4–3.7 Å	3.5–3.7 Å	3.4–3.8 Å
dihedral angle ^[b]	64°	66°	71°	65°	69–74°
ref.	this work	this work	[2]	this work	this work

[a] Dihedral angle between stacking ViPy rings of neighboring molecules. [b] Dihedral angle between bis-chelate fragments of neighboring molecules.

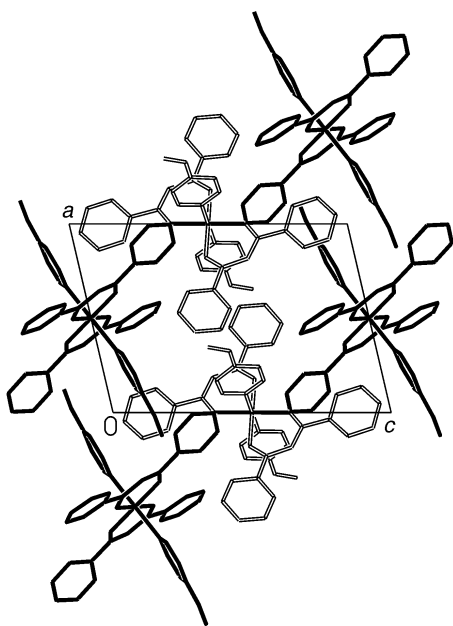


Figure 8. Crystal packing in α' -[Co(4-ViPy)₂(DBM)₂] along *b*. A-molecules are black and B-molecules are white. All the molecules lie on the same level $y \approx 0$.

different from those observed in other structures. The neighboring molecules are interdigitated, being located in the plane and on both sides of the bis-chelate unit. This mode allows metal centers to approach to 9 Å, with an angle between equatorial planes of $\approx 75^\circ$. The shortest distances between metal centers of neighboring chains are from 10 and 11.5 Å.

The α^m -type forms for both Ni and Co complexes, with the two versions very similar. It is monoclinic with four molecules per unit cell and the space group is chiral.^[26] There are two independent molecules (marked A and B), and both are asymmetric. The bischelate fragment is bent in both molecules (Table 6), and the vinyl groups are disordered over two positions. With these specifics, the molecules adopt the same type of conformation as observed in most other phases. There are chains of alternating A and B molecules stretching parallel along the *c* direction (Figure 9). The distances between metal centers in the chain are from 8.2 to 9.4 Å while between the centers of neighboring chains they are >10.2 Å.

Triclinic clathrate types: There are two of these, and both have guest species accommodated in cage-like cavities. Inclusions of Ni- and Co-hosts of the T2 type, [M(4-ViPy)₂(DBM)₂]·2(CCl₄), have two carbon tetrachloride molecules in a prolate spheroidal cage; these structures were described earlier.^[2]

T1-type inclusions form with benzene as guest and a 1:1 host per guest ratio, the Ni- and Co-versions being very similar. The compounds do not lose guest species in air, unlike inclusions of other types, and this is consistent with the inability of guest molecules to diffuse through the structure. There are two centrosymmetric host molecules per unit cell in the structure, and they are crystallographically different (A and B). There are chains of alternating A and B molecules

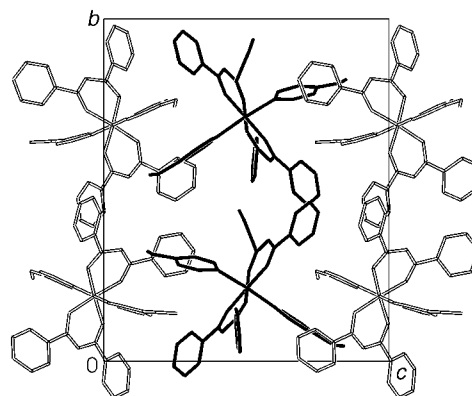


Figure 9. Crystal packing in α^m -[Co(4-ViPy)₂(DBM)₂] along *a*. A-molecules are black and B-molecules are white. The three upper molecules lie on the level of $x \approx 0.75$ and the three lower molecules are at $x \approx 0.25$.

located diagonally between the *a* and *c* directions (Figure 10) with a distance of 8.9 Å between their metal centers. The distance between metal centers of neighboring chains is >10.3 Å. The benzene molecule is located in a cavity formed mainly by pockets of neighboring molecules belonging to different chains, and the fragment was shown in Figure 7b. The inner surface of the cavity is formed by two pyridine and four phenyl moieties from four host molecules. The cut-away section of the structure is shown in Figure 10.

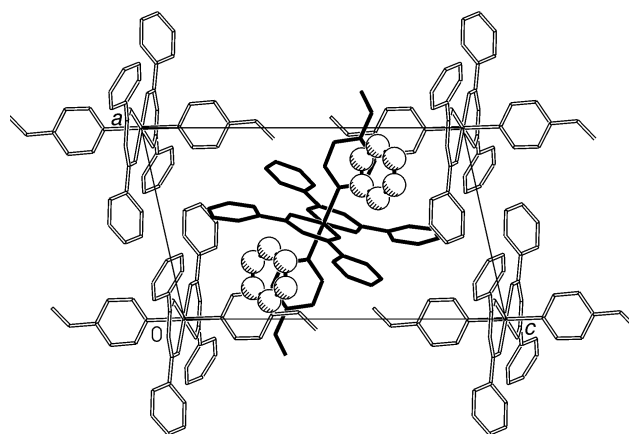


Figure 10. Crystal packing in [Ni(4-ViPy)₂(DBM)₂]·(C₆H₆); cut-away section perpendicular to *b*. The A-molecule is black and B-molecules are white; guest molecules are outlined in sticks-and-balls. Host molecules lie at $y \approx 0$ and guest molecules are at $y \approx 0.25$.

Monoclinic clathrate types: All three monoclinic types, M1, M2 and MC, have guest molecules accommodated in the relatively open cavity space in the form of complex one-dimensional channels with wider and narrower segments. The M1-type was found for Ni- and Co-inclusions with chlorobenzene and a 1:1 host per guest ratio. Some features comparing this type with others are given in Tables 6 and 7, for the remaining details, see our previous work.^[2]

The M2 and MC types are two variations of the same flexible architecture that is evident even from comparison of their powder patterns (Figure 1). Also, as mentioned above, both may transform to the same β polymorph if a guest leaves

very quickly, the β phase probably being akin as well. The conformations of host molecules in these two types are very similar (Table 6) as well as the packing motifs of the molecules (Table 7). The difference lies in the higher symmetry of the MC type that has a C-lattice instead of the P-lattice in M2. The unit cell parameter a in M2 corresponds to the diagonal between a and c in MC while the parameters b comply.

Type M2 forms with methylene chloride guest. The structure of $[\text{Ni}(4\text{-ViPy})_2(\text{DBM})_2] \cdot 2(\text{CH}_2\text{Cl}_2)$ was fully determined and will be discussed; the Co-analogue has a similar composition and unit cell parameters (Table 1). There are four host molecules per unit cell, two are crystallographically different (A and B) and both are centrosymmetric. Chains of alternating A and B molecules lie parallel along the a direction, with a distance between the metal centers of neighboring molecules of 8.9 Å. The distance between metal centers of neighboring chains is >11.7 Å. Guest species are located inside channels extending between chains and parallel to them. The channels are formed by vacant pockets of host molecules belonging to two adjacent chains, and the location of guest species in such pockets is shown in Figure 7. There are two crystallographically different guest molecules; both are disordered (with the occupancy factor of the main orientations 50(2) and 62.3(3)%) and display increased thermal parameters; this suggests significant motional freedom within the excess available space. There are two channels going through the unit cell; they coil about the $(x, \frac{1}{2}, 0)$ and $(x, 0, \frac{1}{2})$ directions with the center forming approximately the figure 8 with a major dimension of ≈ 5.5 Å along b and a minor dimension of ≈ 4 Å along c . The cross-section of the channel perpendicular to the a direction is an ellipse with the sectional area between 18–33 Å²; the shape of the ellipse varies from very oblate (2.5×9.5 Å) to almost round (4.9×5.9 Å). The narrowest passages of 2.5 Å are located at $x=0$ and $a/2$; however, they may open significantly by rotating phenyl rings which control the passages. The fragment of the structure showing three chains forming two channels is given in Figure 11.

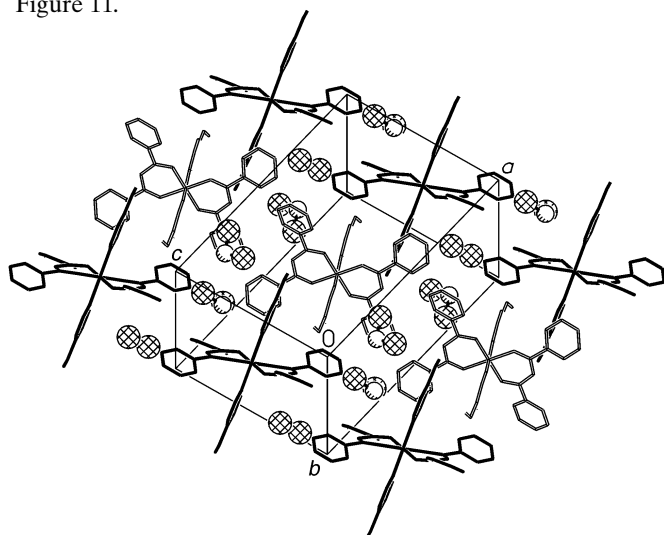


Figure 11. Crystal packing in $[\text{Ni}(4\text{-ViPy})_2(\text{DBM})_2] \cdot 2(\text{CH}_2\text{Cl}_2)$. The A-molecules are black and B-molecules are white; guest molecules are outlined in sticks-and-balls. Three chains lie along a at the level of $y \approx 0.5$; two channels formed by the chains with the accommodated guest species are shown.

Type MC forms for the Ni-host with chloroform, 2-chloropropane, 2-bromopropane, acetone, tetrahydrofuran, nitromethane (Tables 1, 2) and likely with the eight other guests listed in Table 4. The Co-host also forms this type with some of the above guests, and from comparing unit cell dimensions these compounds are similar to the corresponding Ni-compounds (Table 1). Five structures belonging to this type were determined to atomic resolution, four of the Ni-host (with 2-chloropropane, chloroform, acetone and tetrahydrofuran) and one of the Co-host (with nitromethane); for the other five structures only unit cell parameters were measured (Table 1). This type turns out to be very flexible: The range of guests of different shape and polarity results in wide variations of unit cell parameters (a , 19.2–20.2 Å; b , 19.5–19.9 Å; c , 12.4–13.1 Å; V , 4261–4507 Å³). The observed volume variation is thus almost 6%. Only a few systems are known where such a high flexibility accompanies the stability of a specific architecture upon varying the guest type. The best known include the β phases of the Werner complexes,^[19–21] the Hofmann clathrate modifications^[27] and porphyrin-based “sponges”.^[28]

As well as for the M2-type, the unit cell contains four host molecules of which only one is independent. It is centrosymmetric and has a conformation intermediate between the two molecules in the M2-type. The chains of host molecules lie parallel to the diagonal between the a and c directions. The parameters of the chain vary significantly upon changing the guest (Table 7). The best stacking of the vinylpyridine rings is observed for acetone clathrate where the rings are parallel to within 1°. Guest species are located in channels weaving between and parallel to the chains, and are formed by vacant pockets of host molecules belonging to two adjacent chains. The crystal packing, showing three chains and two channels extending between the chains, is given in Figure 12a. Unlike the M2-type, the channel has narrower restrictions of 2.1–2.3 Å controlled also by phenyl rings. There are two channels, four restrictions and eight guest molecules per one unit cell. The restrictions divide channels into wider segments, and every segment is formed mainly by four pockets from four host molecules that incorporates two guest molecules. As may be seen upon viewing the cut-away section of the structure, guest pairs sit in “cradles” which are capped with the next layer above on the b axis. The fragment containing one such “cradle” is shown in Figure 12b. Ideally, two chloroform molecules fit into this “cradle”. In other inclusions of this type, guest species are disordered over two orientations for 2-chloropropane (88.5(4)% for the main orientation), two for acetone (51.3(4)% for the main one), two for nitromethane (51.6(8)% for the main one; Co-host), and three for tetrahydrofuran (63.4(5) and 23.0(6)% for the main ones). To some extent, the “cradle” adjusts its dimensions to the shape and size of a particular guest within certain limits. This provides a structural explanation of the selectivity of the host for certain organic molecules listed in Table 4. The 1:1 stoichiometry suggests that inclusion of n -pentane, n -hexane, n -heptane, 1-chloropentane, 1,2-dimethoxyethane, 2-pentanone, ethyl acetate and diethyl carbonate in the wider segments replaces a pair of smaller guests. This is consistent with approximately the doubled size of the molecules and

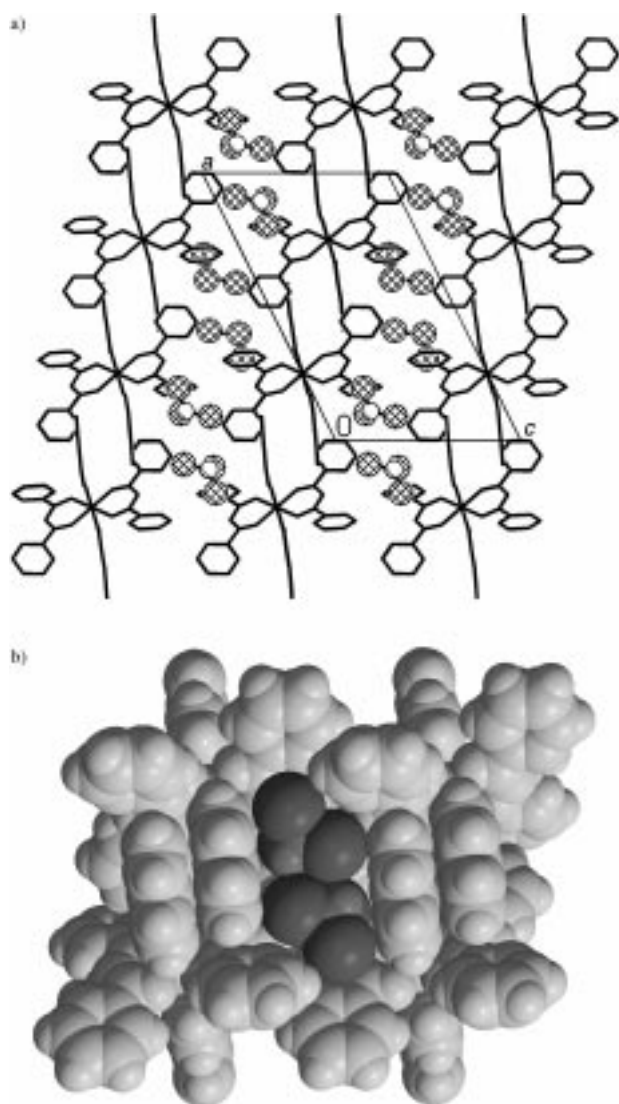


Figure 12. Crystal packing in $[\text{Ni}(4\text{-ViPy})_2(\text{DBM})_2] \cdot 2(\text{CHCl}_3)$ (MC type): a) Packing along b displaying contents between $y=0$ and 0.5 ; host molecules are shown in sticks and guest molecules are outlined in sticks-and-balls. Three host chains and two channels formed by the chains with accommodated guest species are shown. b) Two guest molecules (darkened) sitting in a "cradle" formed by four host molecules; van der Waals dimensions. The fragment corresponds to the right lower part of Figure a).

their linear shape, as shorter or longer molecules, as well as branched isomers are not included.

Conclusion

The main result of the present study is that modification of the parent $[\text{NiPy}_2(\text{DBM})_2]$ host with a vinyl substituent not only retains the clathrate-forming ability of the resulting $[\text{M}(4\text{-ViPy})_2(\text{DBM})_2]$ complex, but enhances it significantly. Of forty organic solvents tested as guests, nineteen were shown to be enclathrated by the new host, and these included unsubstituted and halogenated hydrocarbons, ethers, ketones, aromatic and other compounds. These inclusions belong to five structural types, two with cage and three with channel space available. The addition of rigid substituents to the

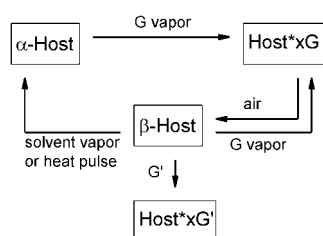
pyridine ring of the host complex gives it more bulkiness and thus should encumber the efficient packing of the molecules. Indeed, this is revealed as a remarkable polymorphism of the title host and its propensity for forming supramolecular architectures. Similarly, the stability and diversity of Werner host $[\text{MA}_4\text{X}_2]$ architectures increases dramatically on going from tetrapyrindine complexes (with pyridine as A)^[24, 29] to complexes with substituted ligands (with ≈ 40 substituted pyridines as A).^[20, 30] Because of this we anticipate excellent prospects for hosts of the metal dibenzoylmethanate type.

The greater clathration ability of $[\text{M}(4\text{-ViPy})_2(\text{DBM})_2]$ is evident also, as most compounds were isolated and analyzed as bulky products, ($[\text{NiPy}_2(\text{DBM})_2]$ often gives mixtures of both host and clathrate phases),^[1] and the inclusion products form readily both from solutions and by interacting the solid host with gaseous guest. From kinetic experiments, even if the host does not form a final inclusion product with a certain guest, the inclusion compound may appear as an intermediate during the polymorphic transformation, thus playing an important role in the process.

The remarkable clathration ability of the title hosts is explainable in terms of the inability of their relatively rigid molecules to form effective packing in three dimensions. In most structures, effective one-dimensional packing motifs were observed for the host molecules implying thereby a packing anisotropy. The presence of small guest molecules strongly facilitates the creation of effective three-dimensional packing. An analogous situation was observed for the $[\text{NiPy}_2(\text{DBM})_2]$ host which shows effective packing in two-dimensional layers but needs a guest component to fill out the cavity space that appears upon stacking these layers in a three-dimensional structure.

As well, this study demonstrates the direct relationship between polymorphism and clathratogenic ability. The polymorphic forms of the host described differ significantly in their ability to form inclusion compounds. The existence of a stable, triclinic α' form for the Co-complex diminishes the range and stability of its inclusions considerably, while isolation of energetically enriched (and seemingly, structurally pre-organized) metastable β form for the Ni-complex makes it possible to accelerate dramatically the inclusion processes and to enclathrate species which do not react with the stable form of the host. The energy difference between guest-free host polymorphs helps to explain the relation in quantitative terms.

The entire study, especially the experiments with the β form, show that factors affecting kinetics, such as initial conditions and catalysis, may play a crucial role in the processes involving the title complexes. The phase interconversion Scheme, as depicted in Scheme 3, reveals the following features. The complete cycle: α form \rightarrow clathrate \rightarrow β form \rightarrow α form may be performed only using the template G (methylene chloride, acetone). As the stable α form cannot be transformed into the β form directly, the cycle may be run only in one direction. Unlike the "passive" α form, the "activated" β form reacts readily with many new guest species (G'). Finally, all the processes proceed quantitatively, do not involve the liquid phase, and are subject to strict control by consecutive application of certain gases or temperature



Scheme 3. Metal–complex host transformations.

conditions. The Scheme gives insight into the potential of flexible host materials for application in highly organized processes, where reproducible changes are controlled not only by applying certain conditions but also by the sequence in which they are applied.

Acknowledgements

We thank L. M. D. Cranswick for alerting us to the program packages combined under the Collaborative Computational Project Number 14 (www.ccp14.ac.uk) within the EPSRC Research Computing Initiative (UK). We thank G. D. Enright for suggesting and consulting on the use of the Microsoft Excel program for minimization procedures, and A. V. Nossov and C. I. Ratcliffe for valuable discussions. D.V.S. is grateful for support in the form of a Visiting Fellowship.

- [1] D. V. Soldatov, G. D. Enright, J. A. Ripmeester, *Supramol. Chem.* **1999**, *11*, 35–47.
- [2] D. V. Soldatov, J. A. Ripmeester, *Supramol. Chem.* **2001**, *12*, 357–368.
- [3] For 3D host matrixes incorporating planar bis-chelate unit see: a) O. Angelova, J. Macicek, M. Atanasov, G. Petrov, *Inorg. Chem.* **1991**, *30*, 1943–1949; b) R. W. Saalfrank, O. Struck, K. Nunn, C. J. Lurz, R. Harbig, K. Peters, H. G. Schnering, E. Bill, A. X. Trautwein, *Chem. Ber.* **1992**, *125*, 2331–2335 (in German); c) for our recent contributions see next reference.
- [4] a) D. V. Soldatov, J. A. Ripmeester, S. I. Shergina, I. E. Sokolov, A. S. Zanina, S. A. Gromilov, Yu. A. Dyadin, *J. Am. Chem. Soc.* **1999**, *121*, 4179–4188; b) D. V. Soldatov, J. A. Ripmeester, *Chem. Mater.* **2000**, *12*, 1827–1839.
- [5] For other bis-chelate hosts see: a) K. A. Fraser, M. M. Harding, *Acta Crystallogr.* **1967**, *22*, 75–81; b) P. J. Squattrito, T. Iwamoto, S. Nishikiori, *Chem. Commun.* **1996**, 2665–2666; c) A. V. Ivanov, M. Kritikos, A. Lund, O. N. Antsutkin, T. A. Rodina, *Russ. J. Inorg. Chem.* **1998**, *43*, 1368–1376.
- [6] A. N. Grigor'ev, M. V. Kiryukhin, L. I. Martynenko, *Russ. J. Inorg. Chem.* **1995**, *40*, 230–233.
- [7] G. M. Sheldrick, *SHELXTL PC, Ver. 4.1. An Integrated System for Solving, Refining and Displaying Crystal Structure from Diffraction Data*, Siemens Analytical X-Ray Instruments, Madison, WI, **1990**.
- [8] E. V. Grachev, Yu. A. Dyadin, J. Lipkowski, *J. Struct. Chem.* **1995**, *36*, 876–879; E. V. Grachev, Yu. A. Dyadin, J. Lipkowski, *Zh. Strukt. Khim.* **1995**, *36*, 956–959 (in Russian).
- [9] E. A. Merritt, D. J. Bacon, *Meth. Enzymol.* **1997**, *277*, 505–524.
- [10] a) Yu. V. Zefirov, P. M. Zorkii, *Russ. Chem. Rev.* **1995**, *64*, 415–428; b) A. Bondi, *J. Phys. Chem.* **1964**, *68*, 441–451.
- [11] H. Irving, R. J. P. Williams, *J. Chem. Soc.* **1953**, 3192–3210.
- [12] a) G. V. Gavrilova, N. V. Kislykh, V. A. Logvinenko, *J. Thermal. Anal. Chem.* **1998**, *33*, 229–235; b) V. A. Logvinenko, D. V. Soldatov, *J. Struct. Chem.* **1998**, *39*, 619–621; V. A. Logvinenko, D. V. Soldatov, *Zh. Strukt. Khim.* **1998**, *39*, 756–760 (in Russian); c) E. A. Ukraintseva, D. V. Soldatov, Yu. A. Dyadin, V. A. Logvinenko, E. V. Grachev, *Mendeleev. Commun.* **1999**, 123–125; d) V. A. Logvinenko, D. V. Soldatov, *J. Thermal. Anal.* **1999**, *56*, 485–492; e) D. V. Soldatov, V. A. Logvinenko, Yu. A. Dyadin, J. Lipkowski, K. Suwinska, *J. Struct. Chem.* **1999**, *40*, 757–771; D. V. Soldatov, V. A. Logvinenko, Yu. A. Dyadin, J. Lipkowski, K. Suwinska, *Zh. Strukt. Khim.* **1999**, *40*, 935–953.
- [13] In some cases the microporous host structures remain intact upon guest removal, and this property is characteristic of zeolites. Other systems displaying such a behavior are often referred to as “zeolite analogues”: a) S. A. Allison, R. M. Barrer, *J. Chem. Soc. A* **1969**, 1717–1723; b) B. T. Ibragimov, S. A. Talipov, T. F. Aripov, *J. Inclusion Phenom.* **1994**, *17*, 317–324; c) A. T. Ung, D. Gizachew, R. Bishop, M. L. Scudder, I. G. Dance, D. C. Craig, *J. Am. Chem. Soc.* **1995**, *117*, 8745–8756; d) M. Kondo, T. Yoshitomi, K. Seki, H. Matsuzaka, S. Kitagawa, *Angew. Chem.* **1997**, *109*, 1844–1846; *Angew. Chem. Int. Ed. Engl.* **1997**, *36*, 1725–1727; e) S. Kitagawa, M. Kondo, *Bull. Chem. Soc. Jpn.* **1998**, *71*, 1739–1753; f) M. Kondo, T. Okubo, A. Asami, S. Noro, T. Yoshitomi, S. Kitagawa, T. Ishii, H. Matsuzaka, K. Seki, *Angew. Chem.* **1999**, *111*, 190–193; *Angew. Chem. Int. Ed.* **1999**, *38*, 140–143; g) C. J. Kepert, M. J. Rosseinsky, *Chem. Commun.* **1999**, 375–376; h) M. Kondo, M. Shimamura, S. Noro, S. Minakoshi, A. Asami, K. Seki, S. Kitagawa, *Chem. Mater.* **2000**, *12*, 1288–1299; i) ref. [4].
- [14] Salient examples of versatile organic hosts displaying extensive polymorphism: Gossipol (seven guest-free polymorphs), see: a) B. T. Ibragimov, S. A. Talipov, *J. Inclusion Phenom.* **1994**, *17*, 325–328; b) M. Gdanec, B. T. Ibragimov, S. A. Talipov in *Comprehensive Supramolecular Chemistry, Vol. 6* (Eds.: D. D. MacNicol, F. Toda, R. Bishop), Pergamon, Oxford, **1996**, p. 117–145; and refs. [48], [68] therein. Hydroquinone (3 guest-free polymorphs): T. C. W. Mak, B. R. F. Bracke, in *Comprehensive Supramolecular Chemistry, Vol. 6* (Eds.: D. D. MacNicol, F. Toda, R. Bishop), Pergamon, Oxford, **1996**, p. 23–60, and refs. [6], [13], [14] therein. 4,5-Bis(4-methoxyphenyl)-2-(4-nitrophenyl)-1H-imidazole (three guest-free polymorphs): Y. Sakaino, R. Fujii, T. Fujiwara, *J. Chem. Soc. Perkin Trans. 1* **1990**, 2852–2854. Perhydrotriphenylene (two guest-free polymorphs): G. Allegra, M. Farina, A. Immirzi, A. Colombo, U. Rossi, R. Broggi, G. Natta, *J. Chem. Soc. B* **1967**, 1020–1028.
- [15] a) H. J. Hart, N. O. Smith, *J. Am. Chem. Soc.* **1962**, *84*, 1816–1819; b) J. Lipkowski, P. Starzewski, W. Zielenkiewicz, *Thermochim. Acta* **1981**, *49*, 269–279.
- [16] J. Lipkowski, J. Chajm, *Rocz. Chem.* **1977**, *51*, 1443–1448.
- [17] D. F. Evans, R. E. Richards, *J. Chem. Soc.* **1952**, 3932–3936.
- [18] a) K. Endo, T. Sawaki, M. Koyanagi, K. Kobayashi, H. Masuda, Y. Aoyama, *J. Am. Chem. Soc.* **1995**, *117*, 8341–8352; b) Y. Aoyama, *Top. Curr. Chem.* **1998**, *198*, 131–161.
- [19] J. Lipkowski, S. Majchrzak, *Rocz. Chem.* **1977**, *49*, 1655–1660.
- [20] a) J. Lipkowski, K. Suwinska, G. D. Andreetti, K. Stadnicka, *J. Mol. Struct.* **1981**, *75*, 101–112; b) J. Lipkowski, in *Inclusion Compounds, Vol. 1* (Eds.: J. L. Atwood, J. E. D. Davies, D. D. MacNicol), Academic Press, London, **1984**, p. 59–103; c) M. H. Moore, L. R. Nassimbeni, M. L. Niven, *J. Chem. Soc. Dalton Trans.* **1987**, 2125–2140; d) J. Lipkowski, *J. Inclusion Phenom.* **1990**, *8*, 439–448; e) L. Lavelle, L. R. Nassimbeni, *J. Inclusion Phenom.* **1993**, *16*, 25–54; f) A. Y. Manakov, J. Lipkowski, K. Suwinska, *J. Inclusion Phenom.* **1996**, *26*, 1–20.
- [21] [Ni(4-MePy)₄(NCS)₂] has two polymorphs: a dense α form a) and a microporous β form b). Both were studied by single-crystal X-ray diffraction method: a) G. D. Andreetti, G. Bocelli, P. Sgarabotto, *Cryst. Struct. Commun.* **1972**, *1*, 51–54; b) I. S. Kerr, D. J. Williams, *Acta Crystallogr. Sect. B* **1977**, *33*, 3589–3592.
- [22] J. Gazo, R. Boca, E. Jona, M. Kabesova, L. Macaskova, J. Sima, P. Pelikan, F. Valach, *Coord. Chem. Rev.* **1982**, *43*, 87–131.
- [23] E. Jona, R. Boca, *J. Inclusion Phenom.* **1992**, *14*, 65–71.
- [24] a) D. V. Soldatov, E. V. Grachev, J. Lipkowski, *J. Struct. Chem.* **1996**, *37*, 658–665; D. V. Soldatov, E. V. Grachev, J. Lipkowski, *Zh. Strukt. Khim.* **1996**, *37*, 764–773 (in Russian); b) D. V. Soldatov, K. Suwinska, J. Lipkowski, A. G. Ogienko, *J. Struct. Chem.* **1999**, *40*, 781–789; D. V. Soldatov, K. Suwinska, J. Lipkowski, A. G. Ogienko, *Zh. Strukt. Khim.* **1999**, *40*, 964–973 (in Russian).
- [25] There are many aromatic rings in the structures and very often they are nearly parallel. Although the distances between atoms of neighboring molecules do not exceed the sum of their van der Waals radii, the presence of weak π – π interactions cannot be excluded.
- [26] The crystal of the Co-complex studied (obtained from toluene) was optically pure (Table 1). All the crystals of the Ni-complex showed twinning; five crystals obtained from four different solvents were

- studied and the refined fractions of the inverted component of the racemic twins were as follows: 0.405(4) for prism ($0.2 \times 0.2 \times 0.5$ mm) from 2,2-dimethoxypropane; 0.45(1) for a piece of a prism ($0.2 \times 0.2 \times 0.2$), also from 2,2-dimethoxypropane; 0.396(9) for a piece of a prism ($0.3 \times 0.5 \times 0.5$) from ethylacetate; 0.476(5) for a block ($0.4 \times 0.5 \times 0.5$) from chlorobenzene; 0.49(1) for a prism ($0.1 \times 0.2 \times 0.3$) from methanol.
- [27] a) T. Iwamoto, *Isr. J. Chem.* **1979**, *18*, 240–245; b) T. Iwamoto, *J. Mol. Struct.* **1981**, *75*, 51–65; c) T. Iwamoto, in *Inclusion Compounds, Vol. 1* (Eds.: J. L. Atwood, J. E. D. Davies, D. D. MacNicol), Academic Press, London, **1984**, p. 29–57; d) T. Iwamoto, *J. Inclusion Phenom.* **1996**, *24*, 61–132.
- [28] a) M. P. Byrn, C. J. Curtis, S. I. Khan, P. A. Sawin, R. Tsurumi, C. E. Strouse, *J. Am. Chem. Soc.* **1990**, *112*, 1865–1874; b) M. P. Byrn, C. J. Curtis, I. Goldberg, Y. Hsiou, S. I. Khan, P. A. Sawin, S. K. Tendick, C. E. Strouse, *J. Am. Chem. Soc.* **1991**, *113*, 6549–6557; c) M. P. Byrn, C. J. Curtis, Y. Hsiou, S. I. Khan, P. A. Sawin, S. K. Tendick, A. Terzis, C. E. Strouse, *J. Am. Chem. Soc.* **1993**, *115*, 9480–9497; d) M. P. Byrn, C. J. Curtis, Y. Hsiou, S. I. Khan, P. A. Sawin, A. Terzis, C. E. Strouse, in *Comprehensive Supramolecular Chemistry, Vol. 6* (Eds.: D. D. MacNicol, F. Toda, R. Bishop), Pergamon, Exeter, **1996**, pp. 715–732.
- [29] a) D. V. Soldatov, J. Lipkowski, *J. Struct. Chem.* **1995**, *36*, 979–982; D. V. Soldatov, J. Lipkowski, *Zh. Strukt. Khim.* **1995**, *36*, 1070–1073 (in Russian); b) D. V. Soldatov, Yu. A. Dyadin, J. Lipkowski, A. G. Ogienko, *Mendeleev Commun.* **1997**, 11–13; c) D. V. Soldatov, Yu. A. Dyadin, J. Lipkowski, K. Suwinska, *Mendeleev Commun.* **1997**, 100–102; d) D. V. Soldatov, J. Lipkowski, *J. Inclusion Phenom.* **1998**, *30*, 99–109; e) D. V. Soldatov, J. A. Ripmeester, *Supramol. Chem.* **1999**, *9*, 175–181.
- [30] J. Lipkowski, in: *Organic Crystal Chemistry* (Eds.: J. B. Garbarczyk, D. W. Jones), Oxford University Press, Oxford, **1991**, pp. 27–35.

Received: November 20, 2000 [F2880]